



The CRL4-DCAF13 ubiquitin E3 ligase supports oocyte meiotic resumption by targeting PTEN degradation

Jue Zhang² · Yin-Li Zhang¹ · Long-Wen Zhao² · Shuai-Bo Pi² · Song-Ying Zhang¹ · Chao Tong² · Heng-Yu Fan^{1,2}

Received: 19 February 2019 / Revised: 31 July 2019 / Accepted: 12 August 2019 / Published online: 6 September 2019
© Springer Nature Switzerland AG 2019

Abstract

Cullin ring-finger ubiquitin ligase 4 (CRL4) has multiple functions in the maintenance of oocyte survival and meiotic cell cycle progression. DCAF13, a novel CRL4 adaptor, is essential for oocyte development. But the mechanisms by which CRL4-DCAF13 supports meiotic maturation remained unclear. In this study, we demonstrated that DCAF13 stimulates the meiotic resumption-coupled activation of protein synthesis in oocytes, partially by maintaining the activity of PI3K signaling pathway. CRL4-DCAF13 targets the polyubiquitination and degradation of PTEN, a lipid phosphatase that inhibits PI3K pathway as well as oocyte growth and maturation. *Dcaf13* knockout in oocytes caused decreased CDK1 activity and impaired meiotic cell cycle progression and chromosome condensation defects. As a result, chromosomes fail to be aligned at the spindle equatorial plate, the spindle assembly checkpoint is activated, and most *Dcaf13* null oocytes are arrested at the prometaphase I. The DCAF13-dependent PTEN degradation mechanism fits in as a missing link between CRL4 ubiquitin E3 ligase and PI3K pathway, both of which are crucial for translational activation during oocyte GV-MII transition.

Keywords Female germ cell · Meiosis · DDB1–CUL4-associated factor 13 · Female fertility · Ubiquitin E3 ligase · PI3K signaling pathway

Introduction

The good quality of oocyte is essential for female fertility [1]. In the post-natal ovaries of mammalian species, fully grown oocytes in follicles are arrested at diplotene stage of the first meiotic prophase, which is also known as the

germinal vesicle (GV) stage [2]. With the stimulation of pituitary gonadotropins in mid-estrus, meiosis resumes with the signature of GV breakdown (GVBD) followed by chromatin condensation [3]. During the prometaphase of meiosis I (Pro-MI), the spindle is assembled accompanied with the capture of condensed chromosomes. When all chromosomes align at the spindle middle plate in the metaphase of meiosis I (MI), the meiotic cell cycle progresses to anaphase I (AI), followed by chromosomes segregation and the exclusion of the polar body-1 (PB1) [4]. Then the ovulated oocytes entered another cell cycle arrest at the metaphase of meiosis II (MII) until fertilization [5]. Errors in meiotic progression result in fertilization failure or abnormalities of preimplantation embryonic development, leading to early abortion and female infertility.

Oocyte meiosis is regulated by a hierarchical network that ensures the normal cell cycle progression and the accurate chromosome separation [6]. Since de novo mRNA transcription ceases in fully grown oocytes, the meiotic maturation, fertilization, and the first embryonic division are completely supported by RNAs and proteins stored in the GV oocytes [7, 8]. Particularly, the progression of oocyte meiosis

Jue Zhang, Yin-Li Zhang, and Long-Wen Zhao contributed equally to this work.

Electronic supplementary material The online version of this article (<https://doi.org/10.1007/s00018-019-03280-5>) contains supplementary material, which is available to authorized users.

✉ Heng-Yu Fan
hyfan@zju.edu.cn

¹ Key Laboratory of Reproductive Dysfunction Management of Zhejiang Province; Assisted Reproduction Unit, Department of Obstetrics and Gynecology, Sir Run Run Shaw Hospital, School of Medicine, Zhejiang University, Hangzhou 310016, China

² MOE Key Laboratory for Biosystems Homeostasis and Protection and Innovation Center for Cell Signaling Network, Life Sciences Institute, Zhejiang University, 866 Yu Hang Tang Rd., Hangzhou 310058, China

requires timely degradation of specific proteins mediated by the ubiquitin- and proteasome-dependent mechanisms.

Protein ubiquitin (Ub) E3 ligases, in particular, play key roles during both meiotic and mitotic cell cycle progression by triggering specific proteins degradation [9]. For example, an anaphase promoting complex (APC) initiates the metaphase–anaphase transition by inducing the degradation of cyclin B and securin [10]. Our previous studies have shown that cullin ring-finger ubiquitin ligase 4 (CRL4) has multiple functions in the maintenance of oocyte survival, meiotic cell cycle progression, and genome reprogramming after fertilization [11]. CRL4 plays versatile biological roles by employing nearly 90 different WD40 repeat-containing adaptor proteins, known as DDB1-cullin-4-associated factors (DCAFs) [12, 13]. These DCAFs recruit a wide spectrum of substrates to CRL4 for poly- or mono-ubiquitylation [14, 15]. DCAF1 and DCAF2 are evolutionarily conserved substrate receptors of CRL4 [16]. Using conditional knockout mouse models, we revealed that both are key mediators of CRL4 function in mammalian oocytes. While DCAF1 regulates the hydroxymethylation of genomic DNA to maintain oocyte survival and to promote zygotic genome reprogramming after fertilization [11, 17, 18], DCAF2 is a previously unrecognized maternal factor that safeguards zygotic genome stability by preventing DNA re-replication in the first mitotic cell cycle of the zygote [19].

In addition to DCAF1 and DCAF2, we recently identified DCAF13 as a novel CRL4 adaptor conserved from yeast to human [20, 21]. DCAF13 is essential for oocyte survival in primordial follicles as well as for preimplantation embryonic development [20, 21]. *Dcaf13* is an early zygotic gene in both murine and human embryos and is expressed mainly at the 8-cell to morula stages. *Dcaf13* knockout murine embryos are arrested at the 8- to 16-cell stage before compaction, and this situation causes preimplantation mortality [21]. To bypass the early embryonic lethality caused by *Dcaf13* knockout, we generated an oocyte-specific *Dcaf13* deletion mouse model, and discovered that this gene plays key roles for oocyte chromatin configuration transition and follicle development [20]. Although CRL4-DCAF13 facilitates genome activation in preimplantation embryos by poly-ubiquitinating and removing the histone H3 lysine-9 (H3K9) trimethylase SUV39H1, this mechanism did not seem to be essential in growing oocytes because the H3K9 trimethylation level did not increase in *Dcaf13* knockout oocytes [20]. Furthermore, analyses of RNA-sequencing results indicated that *Dcaf13* deletion did not significantly affect the transcriptome in oocytes [20]. Therefore, the ubiquitination target proteins of CRL4-DCAF13 in growing oocytes remain obscure.

The *Dcaf13* deletion in oocytes results in a low follicular developmental rate to the antral stage [20]. On the other hand, some of these *Dcaf13* null oocytes can grow to

the GV stage with sizes close to the fully grown wild-type (WT) oocytes, but the females remain sterile. We, therefore, suspected that the *Dcaf13*-deleted oocytes have meiotic maturation defects, and thus failed to be fertilized. In this study, we carefully investigated the meiotic maturation process in *Dcaf13*-deleted oocytes, and demonstrated that the CRL4-DCAF13-regulated biochemical processes are crucial for timely meiotic resumption, normal spindle assembly, accurate chromosome separation, and smooth MI-to-MII transition in maturing mouse oocytes. Mechanistically, CRL4^{DCAF13} targets the polyubiquitination and degradation of PTEN, a lipid phosphatase that inhibits the PI3K pathway as well as oocyte growth and maturation. Therefore, DCAF13 stimulates the meiotic resumption-coupled activation of protein synthesis in oocytes, partially by maintaining the activity of PI3K signaling pathway. These findings not only described novel functions of DCAF13 in supporting oocyte development, but also elucidated a long-looked-for regulation mechanism of PTEN and PI3K signaling pathway in oocytes.

Materials and methods

Oocyte collection and in vitro culture, microinjection

Fully grown oocytes were obtained from the ovaries of 4-week-old *Dcaf13^{fl/fl}* and *Dcaf13^{fl/fl};Gdf9-Cre* female mice 48 h after intraperitoneal injection of 5 IU of PMSG (Ningbo Sansheng Pharmaceutical Co., Ltd., China). Oocytes were released by puncturing follicles with a fine needle in 37 °C pre-warmed M2 medium (Sigma-Aldrich), and cultured in minidrops of M16 medium (M7292; Sigma-Aldrich) covered with mineral oil (M5310; Sigma-Aldrich) at 37 °C in a 5% CO₂ atmosphere. For microinjection, oocytes were collected in M2 medium with 2.5 mM milrinone to inhibit spontaneous GVBD. Flag-DCAF13 mRNAs were transcribed in vitro using a SP6 message machine kit (Invitrogen, AM1450). Microinjection was performed using a micromanipulator and microinjector (Eppendorf) under an inverted microscope (Eclipse TE200; Nikon) as previously described [22]. Approximately 10 pl synthetic mRNA (800 µg/ml) or siRNA (20 µM) diluted in distilled water was microinjected into the cytoplasm of oocytes.

Immunofluorescent staining

Oocytes were fixed with 4% paraformaldehyde in PBS at room temperature for 30 min. They were then permeabilized with 0.3% Triton X-100 in PBS for 30 min. Antibody staining was performed using standard protocols described previously [23]. Antibodies used in the experiments are described

in Supplementary Table 1. Imaging of oocyte was performed on a Zeiss LSM710 confocal microscope. Semi-quantitative analysis of the fluorescence signals was performed through the NIH Image program ImageJ.

Preparation of chromosome spread sections

Oocytes at different meiosis stages were collected and the zona pellucida was removed using acidic M2 medium (pH 2.0). Then oocytes were fixed in a chromosome spread solution (1% paraformaldehyde, 0.15% Triton X-100, and 3 mM dithiothreitol) on glass slides for 1 h. After fixation, slides were air dried. Immunofluorescent staining was performed as done for oocytes as described above.

Detection of protein synthesis

WT and DCAF13-depleted oocytes in growing, fully grown, GVBD, and MI stage were incubated in M16 medium supplemented with 100 mM HPG for 1 h. Then the oocytes were fixed for 30 min at 37 °C in 3.7% formaldehyde. Oocytes were permeabilized in PBS containing 0.5% Triton X-100 for 30 min at room temperature and washed in PBS plus 0.5% Triton X-100. HPG was detected by Click-iT cell reaction kit (Life Technologies). The mean cytoplasmic signal that crossed the middle of each oocyte was measured and quantified using Image-J software.

Western blotting

Oocytes were lysed directly in β -mercaptoethanol containing loading buffer and heated at 95 °C for 10 min. SDS-PAGE and immunoblots were performed following standard procedures using a Mini-PROTEAN Tetra Cell System (Bio-Rad, Hercules, CA). The antibodies used are listed in Supplementary Table 1.

RT-PCR

Quantitative RT-PCR was performed using a Power SYBR Green PCR Master Mix (Applied Biosystems, Life technologies) with ABI 7500 Real-Time PCR system (Applied Biosystems, Life technologies). Relative mRNA levels were calculated by normalizing to the levels of endogenous GAPDH mRNA (used as an internal control). The forward primer 5'-TTTCTGTAGACAAAAGTCGAAGCA-3' and the reward primer 5'-GCATTAGCTTCCACAGGCG-3' were used for *Dcaf13* RT-PCR.

Live cell imaging

In vitro transcribed mRNAs encoding for GFP- α -tubulin and mCherry-securin were microinjected into WT and

DCAF13-deleted oocytes by using an Eppendorf microinjector and released from milrinone after 16 h. Oocytes were cultured in milrinone-free M16 medium containing Hoechst-33342 (to label DNA) within 4 h. Oocytes were subjected to live cell imaging at 12 h after meiotic resumption. Live oocytes were acquired on a DV ELITE High Resolution Invented Living Cell Work station and cultured in M2 medium at 37 °C and 5% CO₂. Image acquisition was performed using Zeiss LSM-780 confocal microscope (Zeiss) equipped with PC-Apochromat 20 \times /0.8 NA objective lenses at 10 min intervals for 12 h.

Cell culture and plasmid transfection

HeLa cells were grown in DMEM (Invitrogen) supplemented with 10% fetal bovine serum (FBS; HyClone) and 1% penicillin–streptomycin solution (Gibco) at 37 °C in a humidified 5% CO₂ incubator. Plasmids were transfected using Lipofectamine 2000 (Invitrogen). The FLAG-DCAF13 plasmids used in our research was described previously [24].

Immunoprecipitation and ubiquitination assay

At 48 h after transfection, Cells were lysed in lysis buffer (50 mM Tris–HCl, pH 7.5, 150 mM NaCl, 10% glycerol, and 0.5% NP-40; protease and phosphatase inhibitors were added prior to use). After centrifugation at 12,000g for 20 min, the supernatant was subjected to immunoprecipitation with an EZview Red Anti-c-Myc affinity gel (Sigma) for 4 h at 4 °C. Then beads were washed three times with lysis buffer. SDS sample buffer was added to the beads. Supernatant (input) and the eluates were used for western blot analysis.

To detect protein ubiquitination status, cells were lysed at 48 h after HA-Ub co-transfection in SDS denaturing buffer (20 mM Tris, pH 7.4, 50 mM NaCl, 0.5% NP-40, 0.5% sodium deoxycholate, 0.5% SDS, and 1 mM EDTA; protein inhibitors were added before use) followed by sonication. Lysate was sonicated and diluted ten times with dilution buffer (50 mM Tris–HCl pH 7.4, 150 mM NaCl, 1 mM EDTA, 0.5% sodium deoxycholate, 1% NP-40, protein inhibitors were added before use). Samples were then incubated with EZview Red anti-HA affinity gel for 2 h at 4 °C, and cleared by centrifuging. Immunoprecipitation assay was detected by western blotting using anti-HA antibody.

Statistical analysis

Results are given as mean \pm SEM. Each experiment was repeated at least three times. Results for two experimental groups were compared by two-tailed unpaired Student's *t* tests. Statistically significant values of $P < 0.05$, $P < 0.01$, and $P < 0.001$ are indicated by asterisks (*), (**), and (***), respectively.

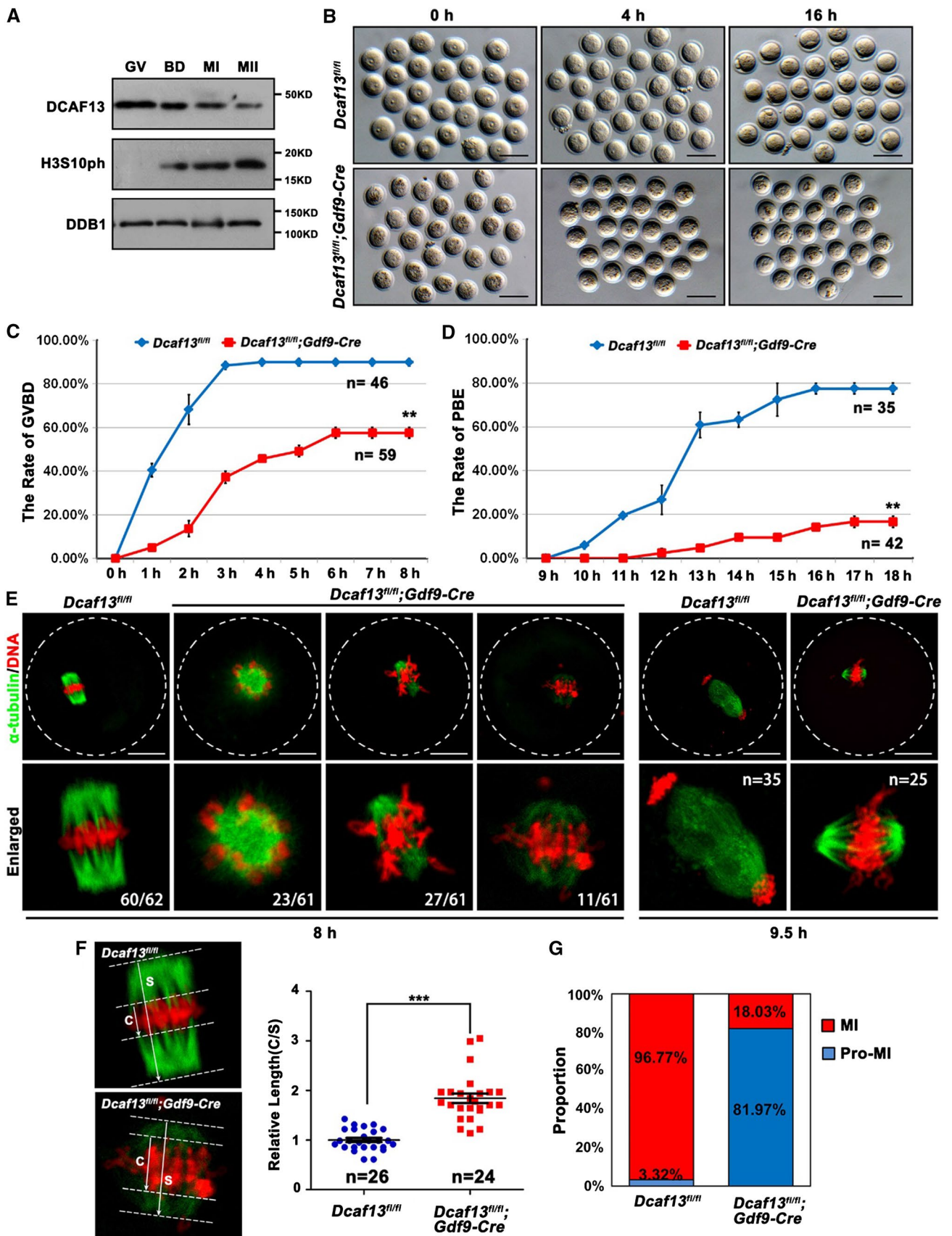


Fig. 1 *Dcaf13* deletion in oocytes impairs meiotic cell cycle progression. **a** Expression of DCAF13 in mouse oocyte as revealed by western blot analysis. DDB1 was blotted as a loading control. Phosphorylation of histone H3 at serine-10 (H3S10ph) was blotted to indicate the levels of chromosome condensation. The sizes (kDa) of protein markers are indicated on the right. **b** Representative images of fully grown oocytes from *Dcaf13^{fl/fl}* and *Dcaf13^{fl/fl};Gdf9-Cre* mice after culture for 0, 4, and 16 h. Scale bar, 100 μ m. **c, d** Germinal vesicle breakdown (GVBD) (**c**) and PB1 emission (PBE) (**d**) rates of cultured oocytes that were collected at the GV stage from mice. Total numbers of oocytes used (*n*) are indicated. ****P**<0.01 by two-tailed Student's *t* tests. Error bars indicate SEM. **e** Immunofluorescence of α -tubulin showing spindles in *Dcaf13^{fl/fl}* and *Dcaf13^{fl/fl};Gdf9-Cre* oocytes after culture for 8 h and 9.5 h. Total numbers of oocytes used are indicated in corner (oocytes showing the representative phenotype/total oocytes being observed). Scale bar, 50 μ m. **f** Measurement of the thickness of spindle middle plate. C indicated maximal span of chromosomes. S indicated maximal spindle lengths. Scatter gram shows the C:S ratios for *Dcaf13^{fl/fl}* and *Dcaf13^{fl/fl};Gdf9-Cre* oocytes after culture for 8 h. Total numbers of oocytes used (*n*) are indicated. *****P**<0.001 by two-tailed Student's *t* tests. Error bars indicate SEM. **g** The proportions of *Dcaf13^{fl/fl}* and *Dcaf13^{fl/fl};Gdf9-Cre* oocytes at Pro-MI and MI stages at 8 h after culture

Results

Dcaf13 deletion in mouse oocytes causes multiple defects of meiotic maturation

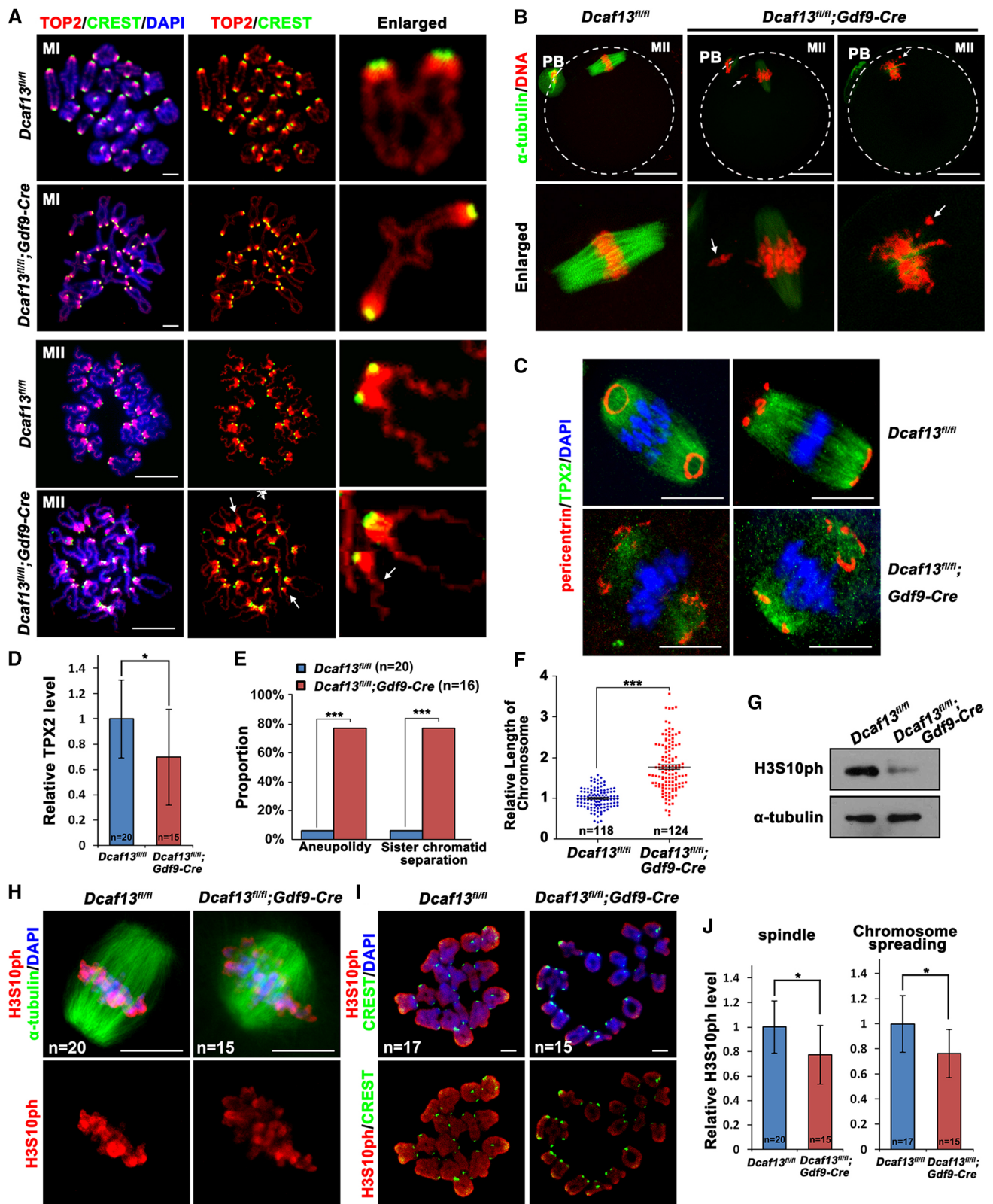
DCAF13 is expressed in mouse oocytes from the primordial follicle stage, so we specifically knocked out *Dcaf13* in oocytes using the well-characterized *Gdf9-Cre*. We have shown in a previous study that DCAF13 protein was deleted as expected in oocytes from primordial follicle stage in *Dcaf13^{fl/fl};Gdf9-Cre* mice through immunohistochemistry and western blotting [20].

DCAF13 was expressed in oocytes throughout the meiotic maturation process, although with a decreasing trend, suggesting that it might potentially be involved in oocyte meiosis (Fig. 1a). To investigate the process of meiotic resumption, we isolated fully grown GV oocytes from pregnant mare serum gonadotropin (PMSG)-primed *Dcaf13^{fl/fl}* (as a control) and *Dcaf13^{fl/fl};Gdf9-Cre* mice and cultured them in vitro. Female mice at the age of 3–4-week-old were used in this study because they have not shown signs of great oocyte loss and premature ovarian failure yet. Oocytes with a diameter greater than 75 μ m were used in the following experiments. Only 57.6% of *Dcaf13*-deleted oocytes underwent GVBD, the first visible sign of meiotic resumption (Fig. 1b, c). Among the oocytes that underwent GVBD within 4 h, only 16.7% extruded the first polar body (PB1) (Fig. 1d). When the control oocytes had formed MI spindles at 8 h after culture, the *Dcaf13*-deleted oocytes contained distorted spindles with weak immunofluorescent signals of α -tubulin and misaligned chromosomes (Fig. 1e). To quantitatively evaluate the extent of chromosome alignment in oocytes, we measured the width of spindle middle plate,

which is the area that is occupied by condensed chromosomes, in relation to the length of the spindle (Fig. 1f). The result showed that the middle plate was significantly broader in *Dcaf13* null oocytes than that in control oocytes. Only less than one-fifth of *Dcaf13*-deleted oocytes developed to MI stage that contained a relatively normal spindle (Fig. 1g).

DCAF13 is crucial for spindle assembly and chromosome condensation during oocyte meiotic divisions

To explain the reason for this phenotype, we observed the spindle assemble and chromosome morphology in *Dcaf13* null oocytes. At 8 h after culture, when the control oocytes have developed to the MI stage, morphological analyses of chromosome spreads indicated that the homologous chromosomes pairing was normal in *Dcaf13*-deleted oocyte (Fig. 2a). Topoisomerase II (TOP2), which is required for chromosome condensation and separation, was normally localized on chromosome arms in both wild type (WT) and *Dcaf13* null oocytes (Fig. 2a). In the *Dcaf13* null oocytes that had released PB1 (less than 20% among oocytes underwent GVBD), the MII spindles were abnormal and the chromosomes were not aligned at the equatorial plates (Fig. 2b). In addition, because TPX2 (targeting protein for the *Xenopus* kinesin *xklp2*) is required for spindle assembly during oocyte maturation, and *Tpx2* depletion causes a phenotype reminiscent of *Dcaf13* knockout [25], we tested if the level of TPX2 is altered in *Dcaf13* null oocytes by immunofluorescence. These new results revealed that TPX2 co-localizes with microtubule on meiotic spindles of WT oocytes (Fig. 2c). Meanwhile, pericentrin, a marker of the microtubule organizing center (MTOC), was detected as rings or dots concentrated at spindle poles (Fig. 2c). In contrast, the TPX2 signal was low and diffused on spindles of *Dcaf13* knockout oocytes (Fig. 2c, d), and pericentrin dots failed to concentrate and merge on spindle poles (Fig. 2c). Following the line that spindle assembly defects can also cause aneuploidy, analyses of chromosome spreadings indicated that their chromosomes were mostly aneuploid and the sister chromatids were precociously separated (Fig. 2a, e). We also found that the chromosome length of *Dcaf13*-deleted oocytes was longer than that of WT oocytes at the MII stage (Fig. 2a, f). Normally, Ser-10 of histone H3 is phosphorylated (H3S10ph) during meiotic resumption. This post-translational histone modification is crucial for chromosome condensation. We compared the level of H3S10ph in control and *Dcaf13*-deleted oocytes cultured for 8 h by western blotting (Fig. 2g) and immunofluorescence (Fig. 2h–j). The results of these experiments indicated a significant decrease in H3S10ph level and a defective chromosome condensation process during meiotic maturation after *Dcaf13* knockout in oocytes.



Overall, these results indicated that *Dcaf13* deletion in oocyte seriously impaired the meiotic maturation process, and caused multiple meiotic division abnormalities

including failure of meiotic resumption, spindle assembly defects, chromosome misalignment, pro-MI arrest, and in some cases, aneuploidy of MII oocytes.

Fig. 2 *Dcaf13* deletion in oocyte cause spindle assembly and chromosome condensation defects. **a** Immunofluorescence results of TOP2 (red) and CREST (green) on chromosomes of *Dcaf13*^{fl/fl} and *Dcaf13*^{fl/fl};*Gdf9-Cre* oocyte showing chromosome arms and centromeres, respectively. Oocytes were subjected to chromosome spreading at 8 h (MI) and 16 h (MII) after culture. Arrows indicate precociously separated chromosomes. Scale bar, 10 μ m. **b** Immunofluorescent staining of α -tubulin in *Dcaf13*^{fl/fl} and *Dcaf13*^{fl/fl};*Gdf9-Cre* oocyte at 16 h after culture. Arrows indicate lagging chromosomes. Scale bar, 50 μ m. **c** Immunofluorescent staining of TPX2 and pericentrin in *Dcaf13*^{fl/fl} and *Dcaf13*^{fl/fl};*Gdf9-Cre* oocyte at 8 h after culture. Scale bar, 50 μ m. **d** Signal intensities of TPX3 in **c**. * $P < 0.05$ by two-tailed Student's *t* tests. Error bars indicate SEM. **e** Rates of MII stage oocytes with chromosome abnormalities including aneuploidy and sister chromatid integrity. *** $P < 0.001$ by two-tailed Student's *t* tests. **f** Quantification of relative chromosome length at MII stage in **a**. Total numbers of chromosomes being measured (*n*) are indicated. **g** Levels of H3S10ph in *Dcaf13*^{fl/fl} and *Dcaf13*^{fl/fl};*Gdf9-Cre* oocyte detected by western blot. Samples of 100 oocytes were collected at 8 h after culture. DDB1 was blotted as a loading control. **h** Immunofluorescence of α -tubulin and H3S10ph in *Dcaf13*^{fl/fl} and *Dcaf13*^{fl/fl};*Gdf9-Cre* oocyte at 8 h after culture. Numbers of oocytes observed are indicated. Scale bar, 10 μ m. **i** Representative images showing H3S10ph (red) and CREST (green) on chromosomes of *Dcaf13*^{fl/fl} and *Dcaf13*^{fl/fl};*Gdf9-Cre* oocyte. Oocytes were subjected to chromosome spreading at 8 h after culture. Scale bar, 10 μ m. **j** Signal intensities of H3S10ph in **h** and **i** normalized by DAPI signals in the same oocytes. * $P < 0.05$ by two-tailed Student's *t* tests. Error bars indicate SEM

Chromosome misalignment in *Dcaf13*-deleted oocyte leads to the activation of spindle assembly checkpoint

During metaphase to anaphase transition in meiosis I, the spindle assembly checkpoint (SAC) prevents chromosome from mis-segregation and aneuploidy [26]. SAC proteins are activated in early metaphase until alignment of all kinetochores on the spindle middle plate. Then the SAC is silenced and the APC^{CDC20} triggers the degradation of securin, followed by chromosome separation and PB1 emission [27]. We observed that BUB3, a core component of SAC which concentrates to the centromeres of control oocyte at the MI stage (8 h after culture), when SAC is active, but becomes undetectable on chromosomes during MI-to-MII transition (9.5 h after culture), when the SAC is inactivated. In comparison, BUB3 was continuously present on the chromosomes of *Dcaf13*-deleted oocytes at both time points (Fig. 3a).

To assess the kinetics of MI-to-MII transition, we micro-injected mRNAs encoding mCherry-securin and GFP- α -tubulin into WT and *Dcaf13*-deleted oocytes and monitored the dynamics of these proteins by epifluorescence. The live cell imaging results (Fig. 3b) revealed that WT oocytes finished meiosis I and developed to MII at 12 h after GVBD. Securin level began to decrease from 6 h post-GVBD and became very low at the anaphase I in control oocytes, but remained stable in *Dcaf13* null oocytes until the end of the

culture (12 h post-GVBD) (Fig. 3b, c). These data suggested that chromosome alignment defects and consequent activation of the SAC blocked APC activation and metaphase-to-anaphase transition, which are marked by securin degradation. This might be the reasons for PB1 emission defect in *Dcaf13* null oocytes.

In the next experiment, we tested if inactivation of SAC could release the *Dcaf13*-deleted oocytes from pro-MI arrest. Control and *Dcaf13* null oocytes were cultured in medium containing a small molecule inhibitor of the SAC protein MPS [28], starting from 2 h post-GVBD. This treatment significantly accelerated PB1 emission in control oocytes, indicating that the MPS inhibitor is effective (Fig. 3d). In MPS inhibitor-treated *Dcaf13* null oocytes, we also observed an acceleration of PB1 emission and an increase of PB1 emission rate. Nonetheless, the PB1 emission rate of these oocytes was still remarkably lower than that of WT oocytes (Fig. 3d). This result suggested that APC^{CDC20} was not active in some *Dcaf13* null oocyte even when SAC was inactivated.

Therefore, we collected the information on whether *Dcaf13* null did or did not release PB1 after MPS inhibitor treatment, and detected the protein levels of CDC20, which is an essential substrate adaptor of APC, and securin, which is a major substrate of APC^{CDC20} in anaphase I [29]. The results show that the CDC20 level was low, and securin was not degraded in *Dcaf13* null oocytes that failed to release PB1 (Fig. 3e). This result confirmed our speculation that a low APC^{CDC20} activity, in addition to a constitutively active SAC, leads to Pro-MI arrest of *Dcaf13*-deleted oocytes.

Restoring CDK1 activity in *Dcaf13*-deleted oocytes rescues meiotic resumption defects

It has been described that there is a dramatic increase in de novo protein (including CDC20 and TPX2) synthesis activity during oocyte meiotic resumption [7, 22, 30]. This GVBD-coupled acceleration of protein synthesis is crucial for the following meiosis events including spindle assembly, chromosome alignment and separation, and PB1 emission [31]. We have shown in previous study that *Dcaf13* deletion in growing oocytes decreases protein translation [20]. Thus, we speculated that the accumulation of proteins essential for meiotic maturation might also depend on a DCAF13-related mechanism.

We incubated WT and *Dcaf13*-deleted oocytes at the GV, GVBD, and Pro-MI stage with L-homopropargylglycine (HPG), an analogue of methionine that can be detected using Click-iT cell reaction kit (Life Technologies), for 1 h. In WT groups, SN oocytes had stronger HPG signals than the NSN oocytes. The HPG signal was elevated significantly after GVBD and then gradually declined (Fig. 4a, b). In comparison, the *Dcaf13*-deleted oocytes had lower HPG signals than those in WT oocytes at the GV and GVBD stages during

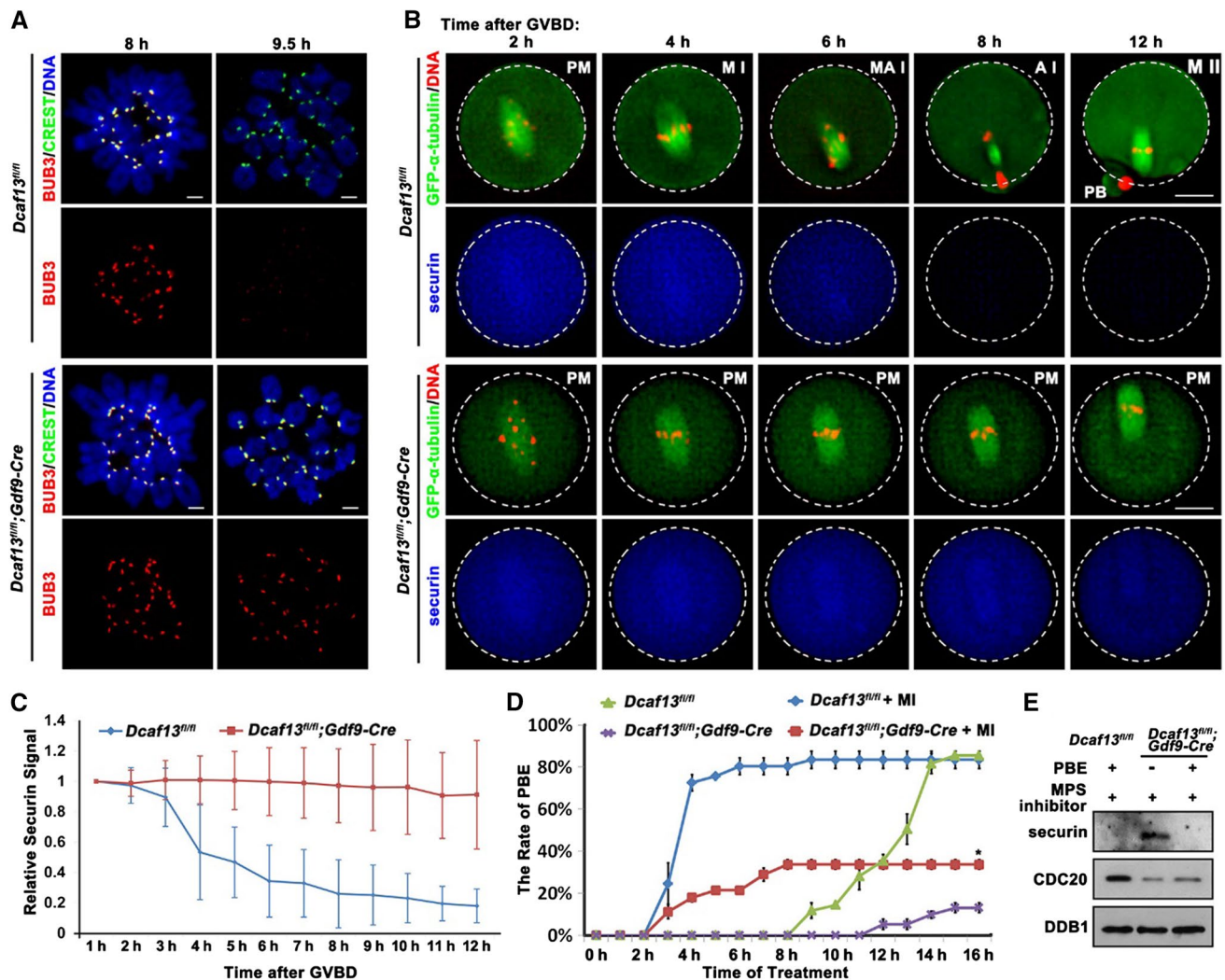


Fig. 3 Role of spindle assembly checkpoint in Pro-MI arrest caused by *Dcaf13* deletion in oocyte. **a** Immunofluorescence results of BUB3 (red) and CREST (green) on chromosome spreads made from *Dcaf13^{fl/fl}* and *Dcaf13^{fl/fl}; Gdf9-Cre* oocytes at 8 and 9.5 h after culture. Scale bar, 10 μ m. **b** GV-arrested oocytes harvested from *Dcaf13^{fl/fl}* and *Dcaf13^{fl/fl}; Gdf9-Cre* mice were co-microinjected with GFP- α -tubulin (to label spindles) and mCherry-securin mRNA. After incubation in M16 containing milrinone for 8 h, microinjected oocytes were transferred to milrinone-free M16 containing Hoechst-33342 (to label DNA), and time-lapse confocal microscopy movies were recorded after GVBD. *PM* pre-metaphase I, *MI* metaphase I, *M-AI* metaphase-anaphase transition, *AI* anaphase I, *MII*

metaphase II. Scale bar, 25 μ m. **c** Quantification of mCherry-securin fluorescence intensity levels in WT (blue) and *Dcaf13*-deleted (red) oocytes at each time point. Time after GVBD is indicated. Values from individual oocytes were normalized relative to that at 1 h. Error bars indicate SEM. **d** PBE rates of *Dcaf13^{fl/fl}* and *Dcaf13^{fl/fl}; Gdf9-Cre* oocytes which were cultured with or without MPS inhibitor (10 μ M) after GVBD. * $P < 0.05$ by two-tailed Student's *t* tests. Error bars indicate SEM. **e** Expressed levels of securin and CDC20 in *Dcaf13^{fl/fl}* and *Dcaf13^{fl/fl}; Gdf9-Cre* oocytes as revealed by western blot. Samples of 100 oocytes were collected after MPS inhibitor treatment for 8 h. Levels of DDB1 were blotted as a loading control

meiotic resumption (Fig. 4a, b). Therefore, the boosted protein translation activation in maturing oocytes fails to occur after *Dcaf13* deletion.

Activation of the key cell cycle regulator CDK1 and accumulation of the CDK1 activators cyclin B1 and CDC25B are prerequisites for GVBD. The CDK1–cyclin B complex is called maturation promoting factor (MPF) [32]. We speculated that the MPF activity might be too low to trigger timely GVBD in *Dcaf13*-deleted oocytes. In oocytes derived from

PMSG-primed *Dcaf13^{fl/fl}* and *Dcaf13^{fl/fl}; Gdf9-Cre* mice, we detected the protein levels of cyclin B1 and CDC25B, which is the phosphatase that removes the inhibitory phosphorylation of CDK1 at Thr-14 and Tyr15 [33], at the GV stage and after cultured for 6 h by western blotting. There were increases in cyclin B1 and CDC25 during meiotic resumption of control oocytes (Fig. 4c). Nonetheless, the levels of these proteins were significantly decreased in *Dcaf13* null oocytes (Fig. 4c). These results indicated that the absence of

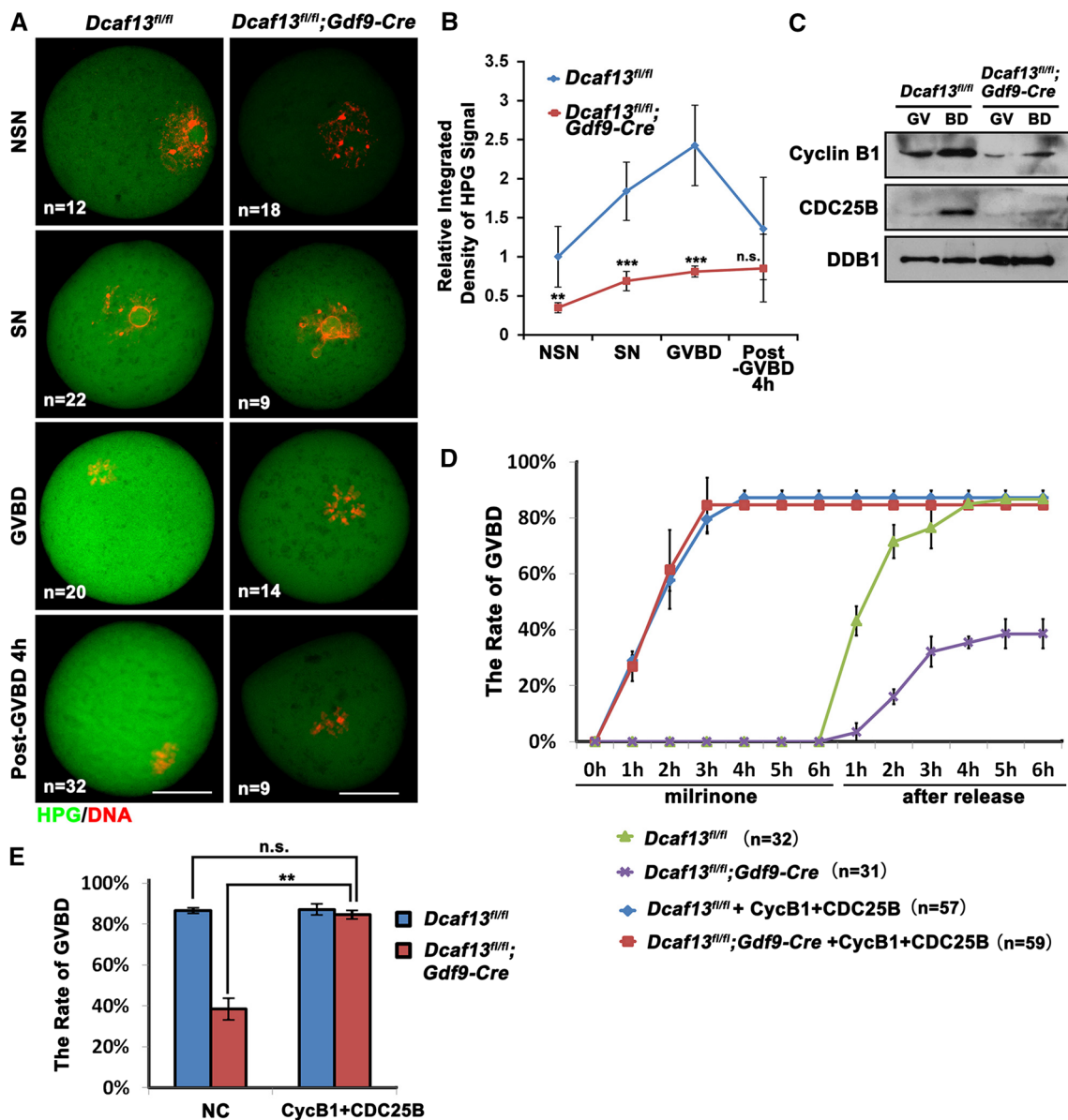


Fig. 4 Levels of protein translation and MPF activity affect the process of meiotic resumption in *Dcaf13*-deleted oocytes. **a** HPG fluorescent staining results showing protein synthesis activity in oocytes at the indicated stages. Oocytes were isolated from 4-week-old *Dcaf13^{fl/fl}* and *Dcaf13^{fl/fl};Gdf9-Cre* mice, and incubated in M2 medium containing 50 μ M HPG for 1 h prior to staining. Total numbers of oocytes used (*n*) in each stage are indicated. Scale bars, 50 μ m. **b** Quantification of HPG signal intensities in **a**. ***P* < 0.01, ****P* < 0.001, by two-tailed Student's *t* tests. Error bars, SEM. **c** Western blot results showing levels of CDC25B and cyclin B1 in

oocytes before and after GVBD. Samples of 100 oocytes were collected before and after culture for 4 h. DDB1 was blotted as a loading control. **d, e** GVBD rates of cultured *Dcaf13^{fl/fl}* and *Dcaf13^{fl/fl};Gdf9-Cre* oocytes that were microinjected with mRNA encoding cyclin B1 and CDC25B or Flag-vector mRNA (as a control) at the GV stage. The microinjected oocytes were incubated in M16 medium containing milrinone for 10 h and then further cultured in milrinone-free medium for 6 h. ***P* < 0.01 by two-tailed Student's *t* tests. *ns* non-significant. Error bars, SEM

protein translation, particularly those related to MPF activation, contributes to meiosis defects after *Dcaf13* depletion.

Then we overexpressed exogenous cyclin B1 and CDC25B [28] in *Dcaf13*-deleted GV oocyte by mRNA microinjection. The oocytes were cultured in M16 medium with 2.5 mM milrinone for 10 h after microinjection. While

uninjected control oocytes resumed the meiotic cell cycle only after being released from milrinone, the oocytes injected with mRNAs encoding cyclin B1 and CDC25B underwent GVBD shortly after microinjection (within 2 h), indicating that the expression of cyclin B1 and CDC25B caused a potent activation of MPF (Fig. 4d). The *Dcaf13*

null oocytes have a similar GVBD rate as the control oocytes after cyclin B1 and CDC25B expression (Fig. 4e). Thus, the decreased CDK1 activity due to insufficient cyclin B1 and CDC25B accumulation was the main cause for the delay of GVBD in oocyte of *Dcaf13^{fl/fl};Gdf9-Cre* mice.

DCAF13 proteins expressed in both growing oocytes and fully grown oocytes contribute to meiotic maturation

In conditional knockout driven by *Gdf9-Cre*, target gene was deleted in oocytes as early as at the primordial follicle stage [34]. Therefore, the defects of meiotic maturation in *Dcaf13* null oocytes might have been caused directly by its

absence during meiotic resumption, or indirectly by abnormalities accumulated during oocyte growth. To investigate if DCAF13 is directly required for meiotic maturation in fully grown GV oocytes in which de novo gene transcription has ceased, we depleted the maternal *Dcaf13* transcripts in well-developed WT GV oocyte by RNA interference (*siDcaf13*) (Fig. 5a) and cultured in vitro for 16 h. The GVBD rate was normal in *siDcaf13* oocyte (Fig. 5b, left panel). Nevertheless, the rate of PB1 emission was lower than control but higher than *Dcaf13* null oocytes derived from *Dcaf13^{fl/fl};Gdf9-Cre* oocyte (Fig. 5b, right panel). We also observed abnormal spindles and misaligned chromosomes in *siDcaf13* oocyte at the MII stage (Fig. 5c, d). These phenotypes are similar to those observed in *Dcaf13* null oocytes.

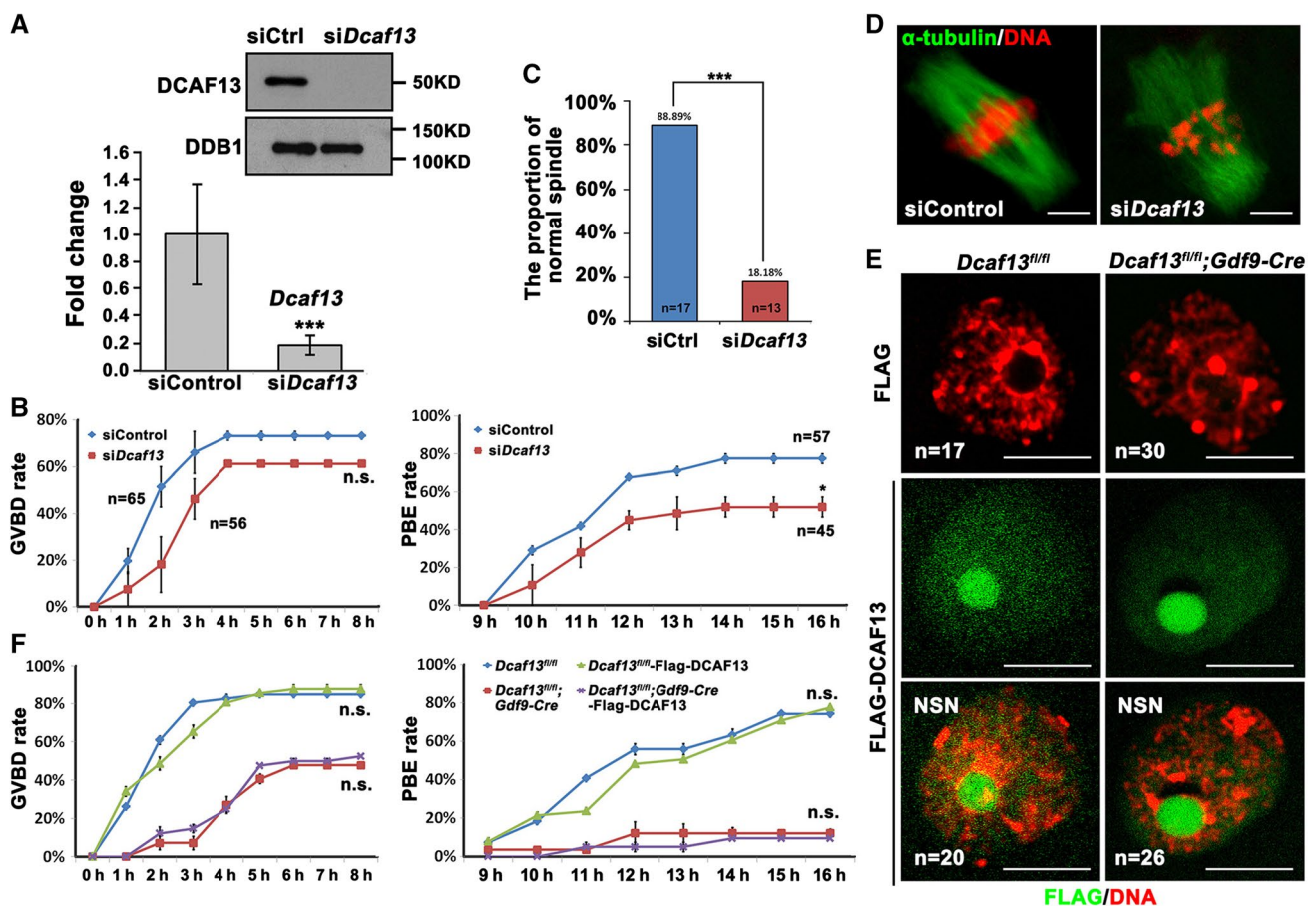


Fig. 5 Effects of *Dcaf13* depletion and overexpression in fully grown oocytes on meiotic maturation. **a** RT-PCR and western blot results showing mRNA and protein levels of *Dcaf13* in oocytes at 16 h after microinjection of *siControl* or *siDcaf13*. The siRNA-microinjected oocytes were held at the GV stage by 2.5 mM milrinone after injection for a period of time (12 h) and then allowed to mature. *** $P < 0.001$, by two-tailed Student's *t* tests. Error bars, SEM. **b** GVBD and PBE rates of oocytes microinjected with *siControl* or *siDcaf13* at the GV stage and further cultured for 16 h. Total numbers of oocytes used (*n*) are indicated. * $P < 0.05$ by two-tailed Student's *t* tests. *ns* non-significant. Error bars indicate SEM. **c** Rate of

oocytes containing a morphological normal spindle after microinjection with *siControl* or *siDcaf13* at the GV stage and further cultured for 16 h. **d** Immunofluorescence of α -tubulin (green) and DNA (red) in oocytes microinjected with *siControl* or *siDcaf13* at the GV stage and further cultured for 16 h. Scale bar, 5 μ m. **e** Immunofluorescence results show the expression of Flag-DCAF13 in GV oocytes. Scale bar, 50 μ m. **f** GVBD and PBE rates of *Dcaf13^{fl/fl}* and *Dcaf13^{fl/fl};Gdf9-Cre* oocytes that were microinjected with mRNAs encoding Flag-DCAF13 or control mRNAs at the GV stage. *ns* non-significant. Error bars indicate SEM.

We also tested if ectopic expression of a Flag-tagged DCAF13 by mRNA microinjection into GV stage-arrested *Dcaf13* null oocytes was able to rescue their meiotic maturation defects. *Dcaf13*^{fl/fl} oocytes were also microinjected as a control group. The expression of Flag-DCAF13 was detected in the GV and nucleolus-like bodies of both *Dcaf13* null and control oocytes by immunofluorescence (Fig. 5e). Then the oocyte was cultured in vitro for 16 h. We found that DCAF13 overexpressed in fully grown GV oocyte had no effect on GVBD and PB1 extrusion both in *Dcaf13*^{fl/fl} and *Dcaf13* null oocyte (Fig. 5f). Collectively, these results suggest that although DCAF13 plays a direct function in regulating meiotic cell cycle progression in fully grown oocytes, DCAF13-dependent mechanisms in growing oocytes are also crucial for establishing the competence of undergoing normal meiotic maturation.

CRL4^{DCAF13} regulates the activation of AKT by targeting PTEN for polyubiquitination and degradation

In the following experiments, we made efforts to elucidate the key mechanism (but of course not the single mechanism, considering the versatile functions of CRL4^{DCAF13}) by which DCAF13 supports oocyte maturation. According to an interactome study in HeLa cells, DCAF13 interacts with PTEN, the well-established repressor of PI3K-AKT signaling pathway [35–37]. Because AKT is involved in CDK1 activation and resumption of meiosis in mouse oocytes [38, 39], we hypothesized that the PI3K-AKT pathway might be afflicted in *Dcaf13* null oocytes.

We tested the phosphorylation levels, which indicate activities, of key factors of PI3K-AKT pathway in growing oocytes, which included AKT (Ser⁴⁷³), p70 ribosome S6 kinase (P70RSK (Thr³⁸⁹)), and RPS6 (Ser^{245/236}) by immunostaining as well as western blot (Fig. 6a–c). We found that the activation levels of these factors were all lower in *Dcaf13* null oocytes compared with those in controls. These observations suggested the biochemical connection between CRL4^{DCAF13} E3 ligase and the PI3K signaling pathway. Because murine oocytes are inconvenient for extensive biochemical analyses, we continued to study biochemical functions of DCAF13 primarily in HeLa cells and then verified the results in oocytes. In agreement with previous data [40], coimmunoprecipitation results showed that DCAF13 and DDB1 interacted with PTEN, when co-expressed in HeLa cells (Fig. 6c). Furthermore, levels of PTEN polyubiquitination significantly increased after DCAF13 or DDB1 overexpression (Fig. 6d). Conversely, when endogenous DCAF13 or DDB1 was depleted by siRNAs, PTEN polyubiquitination levels decreased (Fig. 6e).

To investigate if CRL4^{DCAF13} E3 ligase also regulates PTEN protein level in oocytes, we depleted the *Ddb1* and

Dcaf13 in oocytes by siRNA microinjection and then examined the level of PTEN. Western blot results showed that endogenous PTEN accumulated in WT oocytes after *Ddb1* or *Dcaf13* depletion (Fig. 6f, g). The level of phosphorylated AKT also decreased in *Dcaf13*-knockdown oocytes, presumably as a result of PTEN accumulation (Fig. 6g). On the contrary, the level of PTEN decreased in WT oocytes overexpressing DCAF13 (Fig. 6h). Therefore, we concluded that CRL4^{DCAF13} E3 ligase targets PTEN for polyubiquitination and degradation in both somatic cells and oocytes.

CRL4^{DCAF13}-mediated PTEN degradation is necessary for de novo protein synthesis and meiosis progression in oocytes

Then we tested whether impaired activation of PI3K pathway contributed to oocyte maturation defects caused by *Dcaf13* knockout. When WT oocytes at the GV stage were cultured at the presence of LY-294002, a PI3K inhibitor, about 58% oocytes were arrested at the GV stage and the rate of PB1 was reduced compared with control oocytes (data not shown). The effect of LY294002 is dependent on the concentration and time of treatment. We referred to previous research to identify the concentration of LY294002 (100 μM) that can effectively repress the PI3K pathway while minimizing off-target effects [41]. In another approach, microinjection of mRNAs encoding Flag-PTEN into oocytes decreased the activation of AKT (Fig. 7a) and the rates of GVBD (Fig. 7b). Despite PB1 emission rate was not affected (Fig. 7c), the PTEN-overexpressing oocytes contained distorted spindles and misaligned chromosomes (Fig. 7d). Moreover, overexpression of PTEN, as well as incubation with LY-294002, caused decreases in protein synthesis activity in oocytes (Fig. 7e, f) and defects of MI spindle assembly (Fig. 7g). TPX2 is a protein transiently synthesized during oocyte maturation and is essential for spindle assembly and chromosome interaction with microtubules [7]. The level of TPX2 expression is critical for spindle function [42]. However, in the LY-294002-treated oocytes or PTEN-overexpression oocytes, the level of TPX2 on the meiotic spindle was lower than control (Fig. 7g). These phenotypes partially mimicked those caused by *Dcaf13* knockout in oocytes, suggesting that the decreased activity of PI3K pathway is an important reason that contributes to meiotic maturation defects in *Dcaf13*-null oocytes.

Discussion

The gene encoding DCAF13 was first discovered in yeast in 2003 [43], and was later shown to be evolutionarily conserved and to perform key functions in the preimplantation embryos. CRL4^{DCAF13} interacts with the histone

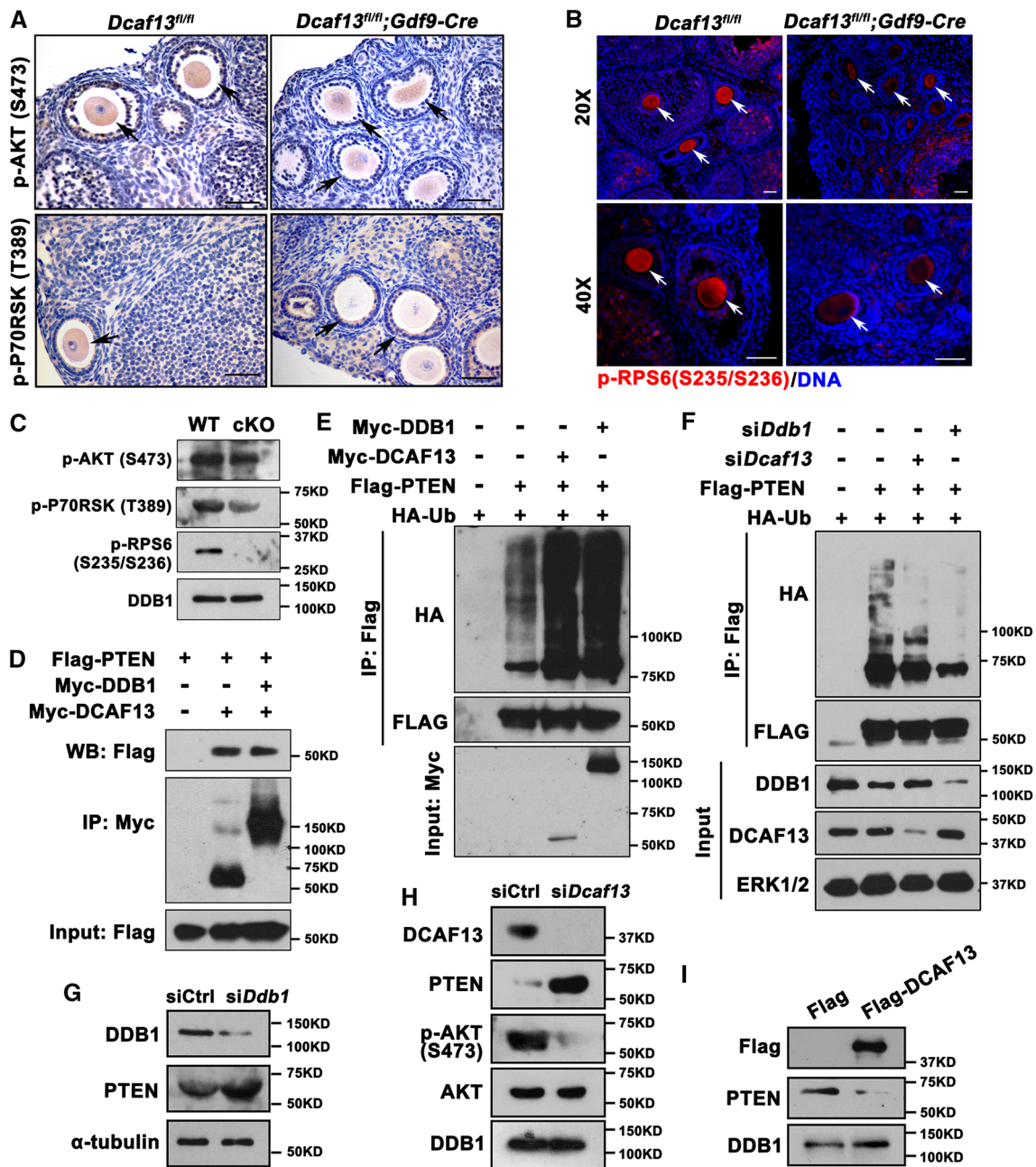


Fig. 6 CRL4^{DCAF13} targets PTEN for polyubiquitination and degradation. **a–c** Immunohistochemistry (**a**), immunofluorescence (**b**), and western blot (**c**) results showing the level of phosphorylated AKT (Ser⁴⁷³), p70 ribosome S6 kinase (P70RSK-Thr³⁸⁹), and RPS6 (Ser^{245/236}) in oocytes of 4-week-old mice with indicated genotypes. Arrows indicate growing oocytes. Scale bars, 50 μ m. **d** Co-immunoprecipitation result showing PTEN interaction with DCAF13 and DDB1. HeLa cells were co-transfected with Flag-PTEN and Myc-DCAF13 or Myc-DDB1 expression plasmids for 24 h. Target proteins were immunoprecipitated using anti-Myc beads and subjected to western blotting with FLAG and Myc antibodies. Input cell lysates were immunoblotted with an anti-Flag antibody to determine the expression of PTEN. **e** HeLa cells transiently transfected with plasmids encoding the indicated proteins were lysed and subjected to

immunoprecipitation with an anti-HA affinity gel. Input cell lysates and precipitates were immunoblotted with antibodies against FLAG, HA, and MYC. **f** Co-IP followed by western blotting showing PTEN polyubiquitination in control HeLa cells and those transfected with *Dcaf13* or *Ddb1* siRNAs. **g** Western blotting results showing the levels of PTEN in oocytes microinjected with control siRNA (siCtrl) or siDdb1. α -Tubulin was blotted as a loading control. **h** Western blotting results showing the levels of PTEN, AKT, and phosphor-AKT (Ser⁴⁷³) in oocytes after microinjected with siControl or siDcaf13 and further cultured for 36 h. DDB1 was blotted as a loading control. **i** Western blotting results showing the levels of PTEN in oocytes after microinjected with Flag-vector or Flag-DCAF13 mRNA and further cultured for 24 h. DDB1 was blotted as a loading control. Sizes (kDa) of protein markers are indicated on the right in all figures

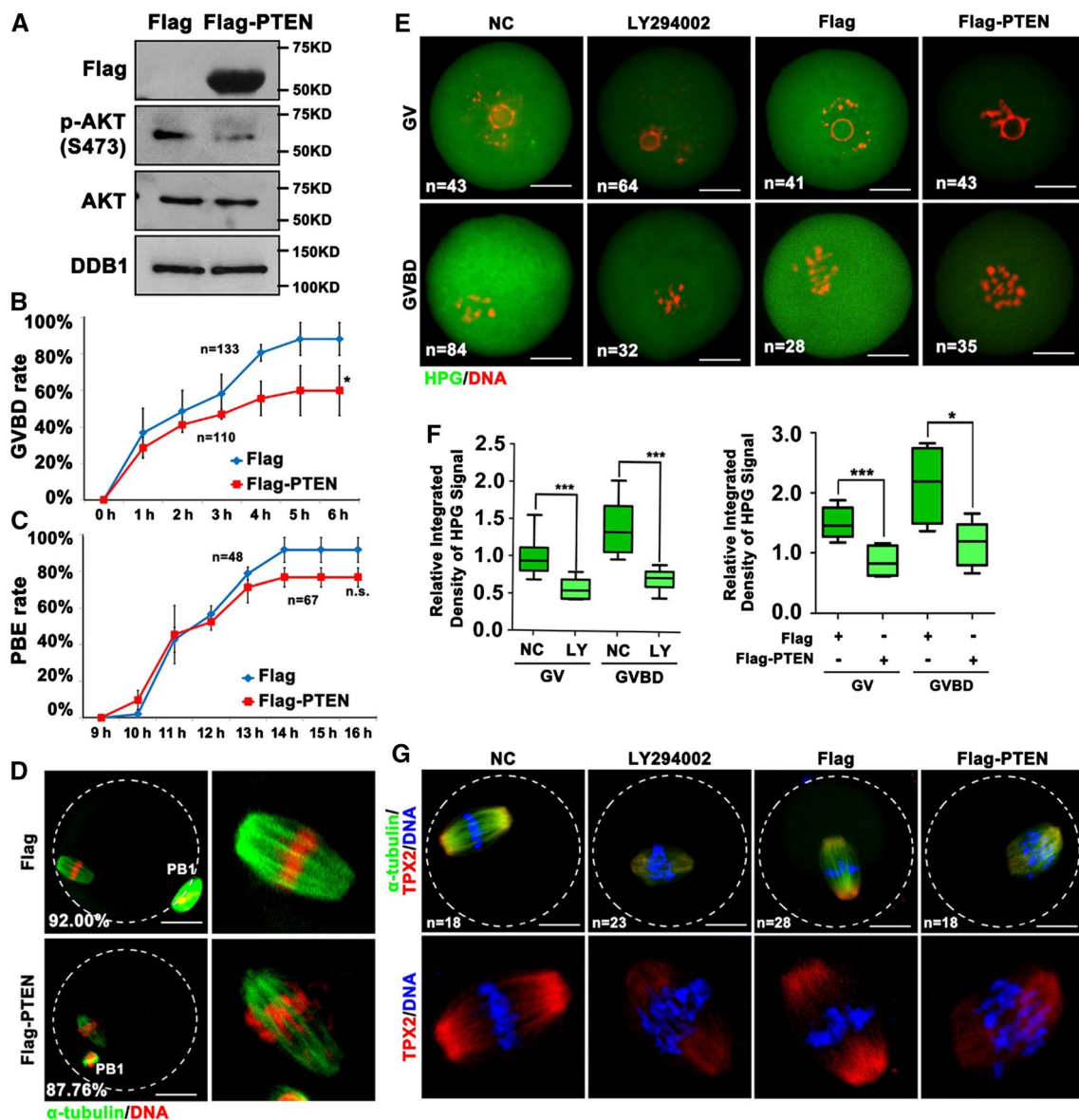


Fig. 7 PTEN overexpression affected oocytes meiotic resumption and levels of protein translation. **a** Western blotting results showing the levels of AKT and phosphor-AKT (Ser⁴⁷³) in oocytes after microinjected with Flag-vector or Flag-PTEN mRNA at the GV stage and further cultured for 24 h. Sizes (kDa) of protein markers are indicated on the right. **b**, **c** GVBD (**b**) and PBE emission (**c**) rates of oocytes that were microinjected with Flag-vector or Flag-PTEN mRNA at the GV stage. Total numbers of oocytes used (*n*) are indicated. **P* < 0.05 by two-tailed Student's *t* tests. Error bars indicate SEM. **d** Immunofluorescence of α -tubulin showing spindles in oocytes microinjected with Flag-vector or Flag-PTEN mRNA at the GV stage after culture for 16 h. Scale bar, 50 μ m. The rate of spindle assembly of oocytes

are shown in corner. **e** HPG fluorescent staining results showing protein synthesis activity in oocytes. Oocytes were isolated from 3 to 4-week-old WT mice, incubated with or without LY294002 for 2 h; or microinjected with mRNAs encoding Flag-PTEN. Then oocytes were incubated in M2 medium containing 50 μ M HPG for 1 h prior to staining. Total numbers of oocytes used (*n*) in each stage are indicated. Scale bars, 50 μ m. **f** Quantification of HPG signal intensities in (e). **P* < 0.05, ****P* < 0.001 by two-tailed Student's *t* tests. Error bars indicate SEM. **g** Immunofluorescence results showing the level of TPX2 in oocytes treated with LY294002 or microinjected with Flag-PTEN mRNAs and then further cultured for 8 h. Total numbers of oocytes used are indicated in corner. Scale bar, 50 μ m

methyltransferase SUV39H1 and directs it to polyubiquitination and proteasomal degradation, and therefore facilitates the removal of trimethylated histone H3 at lysine-9 and early zygotic gene expression. On the other hand, its participation in post-natal development and hemostasis was not studied

in the first report, owing to the early mortality of *Dcaf13* knockout embryos at the 8–16-cell stage.

After generating a novel *Dcaf13*-floxed mouse strain, we studied the function of *Dcaf13* in oogenesis by knocking out this gene in oocyte using *Zp3-Cre*. In growing oocytes,

nucleolus-localized DCAF13 is an important component of the ribosomal RNA (rRNA)-processing complex. DCAF13 deletion in oocytes led to follicle growth retardation, impaired NSN-SN configuration transition, and ultimately caused POF. Further exploration showed that DCAF13 participates in the 18S rRNA processing in growing oocytes. The lack of 18S rRNA caused a ribosome assembly disorder and then reduced global protein synthesis [20]. In addition, the zygotes derived from these defective oocytes do not have developmental potential and are arrested at the 2-cell stage after fertilization, most likely because the transcription activation of zygotic genome failed to occur [44].

However, the biochemical function of DCAF13, as an adaptor subunit of CRL4 ubiquitin E3 ligase, in mediating target protein degradation, has been investigated in oocytes. Maternal *Dcaf13* knockout inhibited protein synthesis, but had little impact on mRNA transcription and histone methylation levels in oocytes [20]. These observations suggested that DCAF13 functions in oocytes by mechanisms other than targeting the histone methyltransferase SUV39H1 for degradation.

In this study, we further demonstrated that DCAF13 is required for normal meiotic cell cycle progression of oocytes. To assess the impact of *Dcaf13* knockout on meiotic maturation, which is an event later than intrafollicular oocyte growth, we isolated GV oocytes from 4-week-old *Dcaf13^{fl/fl};Gdf9-Cre* female mice for analyses. At this young age, these mice have not shown obvious signs of premature ovarian insufficiency. Therefore, we were able to harvest fully grown oocytes from the ovaries, although the numbers are fewer than normal.

Oocyte meiotic resumption is accompanied by a remarkable increase in protein synthesis. These temporally translated proteins play key roles in the principal meiotic events, such as reorganization of microtubules, meiotic spindle assembly, condensation and segregation of chromosomes, as well as meiosis II (MII) arrest [45]. Therefore, the quality of oocyte meiotic maturation is to a large extent dependent on protein synthesis as the regulation of gene expression at the transcription level at the meiosis stage is halted [30]. Our current results indicated that DCAF13 expressed in both growing and fully grown oocytes are crucial for the translation of key meiosis regulators including cyclin B1, CDC25B, and CDC20. Both cyclin B and CDC25B are important to activate CDK1 during meiotic resumption. It is well recognized that CDK1 activity is essential to maintain the chromosomes in a condensed state during oocyte maturation. Therefore, decreased cyclin B1 and CDC25B levels may be the cause of chromosome condensation defect in *Dcaf13* knockout oocytes.

Based on our recent findings, DCAF13 might ensure adequate global protein translation activity of maturing oocytes by regulating rRNA synthesis and ribosome assembly during

oocyte growth [20]. Although DCAF13 is enriched in nucleolus-like bodies in oocytes and early embryos, this CRL4 adaptor is also detected in the neoplasm, suggesting that it also has nucleolus-independent function. In addition, the fact that depletion of DCAF13 in transcriptionally inactive GV oocytes also impaired meiosis indicates DCAF13 has a direct function in meiotic maturation in addition to indirectly stimulating rRNA transcription and splicing.

To elucidate the underlying mechanisms, we searched the human protein interactome and noticed the potential interaction between DCAF13 and PTEN, the key inhibitor of PI3K pathway. This observation enlightened us because it has been reported that PI3K pathway triggers meiotic cell cycle progression in oocytes by multiple mechanisms [38, 39, 41, 46]. Results of further experiments collectively established that CRL4^{DCAF13} maintains PTEN protein at a low level by mediating their polyubiquitination and degradation, and PTEN accumulation led to defective protein synthesis and meiotic maturation in oocytes. These two *Dcaf13*-dependent mechanisms (rRNA synthesis and PTEN degradation) are not exclusive to each other, and may both contribute to the physiological importance of DCAF13 in oogenesis. This finding also answered a long-standing question of how the activity of PI3K signaling pathway, particularly the abundance of PTEN protein level, is regulated by intraoocyte factors.

This question was raised as early as more than a decade ago when the fundamental role of PI3K pathway in oocyte growth and maturation was beginning to be recognized. PI3K activation plays an important role in growth factor-dependent oocyte meiotic maturation. Inhibition of PI3K as well as AKT, the key kinase in PI3K pathway, in maturing oocytes impaired GVBD, spindle assembly, and chromosome alignment [41, 46–50]. AKT directly phosphorylates and activates cGMP-inhibited cAMP phosphodiesterase 3A (PDE3A), which is essential for meiotic resumption of GV stage-arrested oocytes [39]. Furthermore, translation of a subset of oocyte mRNAs is under the control of somatic cell inputs acting through the PI(3)K pathway [38]. These regulation functions are involved in establishing the competence of oocytes to accomplish meiotic maturation. However, the mechanism that regulates PI3K/AKT activity in oocytes was not investigated before we identified the CRL4^{DCAF13}-mediated PTEN degradation pathway. Two recent studies reported that DCAF13 expression was upregulated in human osteosarcoma cells and hepatocellular carcinoma samples [40, 51]. Employing multivariate Cox regression analysis, these authors showed that DCAF13 was a prognostic predictor of survival in hepatocellular carcinoma patients [51]. They suggest that DCAF13 is a potential cell cycle regulator. Disrupting the stability of CRL4B^{DCAF13} E3 ligase by small molecules resulted in PTEN accumulation and greatly inhibited osteosarcoma cell growth [40].

Consistent with this finding but at an advantage of using an in vivo model system, we demonstrated that DCAF13 was involved in meiotic division based on its regulation of protein synthesis potentially by removing PTEN and activating PI3K pathways (Fig. 8).

The results of this study also shed light on the mechanism that associated with our recent work in which we describe a DCAF13 downregulation-associated functional decline of the oocyte quality and developmental potential. In that study, we reported that proper rRNA synthesis and ribosome accumulation mediated by DCAF13 and its associated nucleolar proteins, such as fibrillarin, are prerequisites of translational activation during oocyte GV-MII transition [20]. Nevertheless, how does oocyte DCAF13, as one of substrate receptors of the CRL4 complex, perform an E3 ubiquitin ligase function in regulating follicular development was unexplained. The discovery that CRL4^{DCAF13} maintains an appropriate activity of PI3K pathway in oocytes logically fits in its role

in developing follicles. Activity of PI3K pathway is required for primordial follicle activation, follicle growth, and maintenance [52, 53]. PTEN is highly expressed in oocytes at the primordial follicle stage and represses their awakening [36]. By mechanisms previously unclear, PTEN's inhibitory effect was relieved in some oocytes. Then these oocytes enter the pool of growing follicles. DCAF13 is strongly expressed in growing follicles, and may provide a key intracellular signal that facilitates the partial removal of PTEN and maintains a high activity of PI3K signaling. The phenotype of *Dcaf13* knockout in oocytes (retarded follicle growth and premature ovarian insufficiency) partially mimics those of *Pdk1* and *Rps6* knockout (both genes encode key components of PI3K pathway) [54], suggesting that CRL4^{DCAF13}-mediated PTEN degradation is also a permissive mechanism for normal follicle development.

Collectively, in this study, we described meiotic maturation-related phenotypes observed in oocyte-specific *Dcaf13*

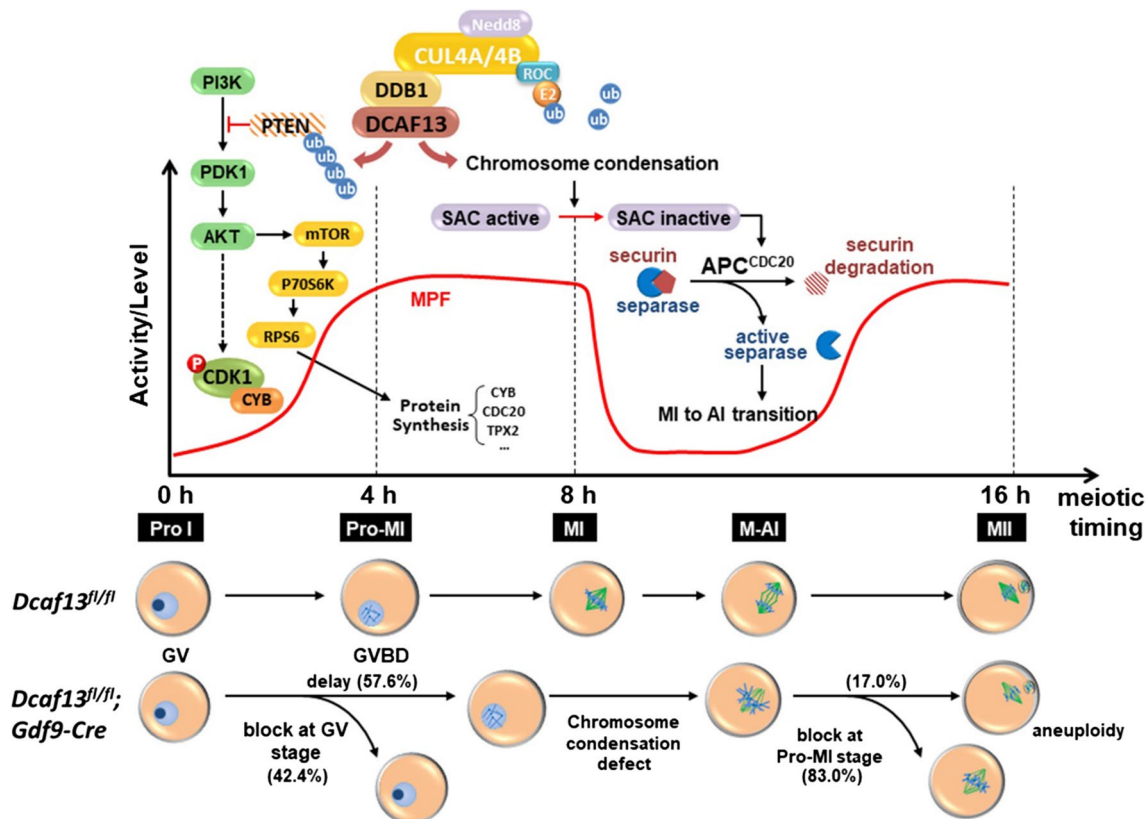


Fig. 8 A diagram showing the role of DCAF13 in oocyte meiotic maturation. DCAF13 is required to maintain normal protein synthesis activity in maturing oocytes. During meiosis resumption stage, CRL4^{DCAF13} facilitates the activation of AKT by targeting PTEN for polyubiquitination and degradation, which promotes the translation of Cyclin B1 and TPX2 and the activation of MPF. *Dcaf13* knockout in oocytes caused decreased MPF activity and impaired meiotic cell cycle progression including GV arrest, delayed GVBD, and chromosome condensation defects. As a result, chromosomes fail to

be properly aligned at the spindle middle plate, the spindle assembly checkpoint is activated, and most *Dcaf13* null oocytes are arrested at the prometaphase I. In addition, insufficient accumulation of CDC20 proteins also impairs the activation of anaphase promoting complex (APC) and prevents the metaphase-to-anaphase transition in meiosis I. Even a small portion of *Dcaf13* null oocytes can release PB1 and develop to MII, and they have a high rate of aneuploidy due to accumulated meiotic abnormalities

knockout mice (Fig. 8) in addition to the defects of follicle development. We also identified PTEN, an important PI3K pathway regulator and a well-established tumor repressor, as intraoocyte target of CRL4^{DCAF13} ubiquitin E3 ligase. These physiological as well as biochemical findings extend the current understanding of oocyte development regulation. The same mechanism may also potentially crucial in some other developmental processes and cancer development.

Acknowledgements This study is funded by the National Key Research and Developmental Program of China (2017YFC1001100, 2017YFC1001500, 2016YFC1000600), National Natural Science Foundation of China (31528016, 31671558), and The Key Research and Development Program of Zhejiang Province (2017C03022).

Compliance with ethical standards

Conflict of interest The authors declare no competing interest.

References

- Zuccotti M, Giorgi Rossi P, Martinez A, Garagna S, Forabosco A, Redi CA (1998) Meiotic and developmental competence of mouse antral oocytes. *Biol Reprod* 58(3):700–704
- Tan JH, Wang HL, Sun XS, Liu Y, Sui HS, Zhang J (2009) Chromatin configurations in the germinal vesicle of mammalian oocytes. *Mol Hum Reprod* 15(1):1–9. <https://doi.org/10.1093/molehr/gan069>
- Mehlmann LM (2005) Stops and starts in mammalian oocytes: recent advances in understanding the regulation of meiotic arrest and oocyte maturation. *Reproduction* 130(6):791–799. <https://doi.org/10.1530/rep.1.00793>
- Sun SC, Kim NH (2013) Molecular mechanisms of asymmetric division in oocytes. *Microsc Microanal* 19(4):883–897. <https://doi.org/10.1017/S1431927613001566>
- Pan B, Li J (2019) The art of oocyte meiotic arrest regulation. *Reprod Biol Endocrinol* 17(1):8. <https://doi.org/10.1186/s12958-018-0445-8>
- Li XM, Yu C, Wang ZW, Zhang YL, Liu XM, Zhou D, Sun QY, Fan HY (2013) DNA topoisomerase II is dispensable for oocyte meiotic resumption but is essential for meiotic chromosome condensation and separation in mice. *Biol Reprod* 89(5):118. <https://doi.org/10.1095/biolreprod.113.110692>
- Sha QQ, Dai XX, Dang Y, Tang F, Liu J, Zhang YL, Fan HY (2017) A MAPK cascade couples maternal mRNA translation and degradation to meiotic cell cycle progression in mouse oocytes. *Development* 144(3):452–463. <https://doi.org/10.1242/dev.144410>
- Dai XX, Jiang JC, Sha QQ, Jiang Y, Ou XH, Fan HY (2018) A combinatorial code for mRNA 3'-UTR-mediated translational control in the mouse oocyte. *Nucleic Acids Res*. <https://doi.org/10.1093/nar/gky971>
- Huo LJ, Fan HY, Liang CG, Yu LZ, Zhong ZS, Chen DY, Sun QY (2004) Regulation of ubiquitin-proteasome pathway on pig oocyte meiotic maturation and fertilization. *Biol Reprod* 71(3):853–862. <https://doi.org/10.1095/biolreprod.104.028134>
- Jones KT (2011) Anaphase-promoting complex control in female mouse meiosis. *Results Probl Cell Differ* 53:343–363. https://doi.org/10.1007/978-3-642-19065-0_15
- Yu C, Zhang YL, Pan WW, Li XM, Wang ZW, Ge ZJ, Zhou JJ, Cang Y, Tong C, Sun QY, Fan HY (2013) CRL4 complex regulates mammalian oocyte survival and reprogramming by activation of TET proteins. *Science* 342(6165):1518–1521. <https://doi.org/10.1126/science.1244587>
- Lee J, Zhou P (2007) DCAFs, the missing link of the CUL4-DDB1 ubiquitin ligase. *Mol Cell* 26(6):775–780. <https://doi.org/10.1016/j.molcel.2007.06.001>
- Iovine B, Iannella ML, Bevilacqua MA (2011) Damage-specific DNA binding protein 1 (DDB1): a protein with a wide range of functions. *Int J Biochem Cell Biol* 43(12):1664–1667. <https://doi.org/10.1016/j.biocel.2011.09.001>
- Emanuele MJ, Elia AE, Xu Q, Thoma CR, Izhar L, Leng Y, Guo A, Chen YN, Rush J, Hsu PW, Yen HC, Elledge SJ (2011) Global identification of modular cullin-RING ligase substrates. *Cell* 147(2):459–474. <https://doi.org/10.1016/j.cell.2011.09.019>
- Bennett EJ, Rush J, Gygi SP, Harper JW (2010) Dynamics of cullin-RING ubiquitin ligase network revealed by systematic quantitative proteomics. *Cell* 143(6):951–965. <https://doi.org/10.1016/j.cell.2010.11.017>
- Pan WW, Zhou JJ, Yu C, Xu Y, Guo LJ, Zhang HY, Zhou D, Song FZ, Fan HY (2013) Ubiquitin E3 ligase CRL4(CDT2/DCAF2) as a potential chemotherapeutic target for ovarian surface epithelial cancer. *J Biol Chem* 288(41):29680–29691. <https://doi.org/10.1074/jbc.M113.495069>
- Yu C, Ji SY, Sha QQ, Sun QY, Fan HY (2015) CRL4-DCAF1 ubiquitin E3 ligase directs protein phosphatase 2A degradation to control oocyte meiotic maturation. *Nat Commun* 6:8017. <https://doi.org/10.1038/ncomms9017>
- Yu C, Xu YW, Sha QQ, Fan HY (2015) CRL4DCAF1 is required in activated oocytes for follicle maintenance and ovulation. *Mol Hum Reprod* 21(2):195–205. <https://doi.org/10.1093/molehr/gau103>
- Xu YW, Cao LR, Wang M, Xu Y, Wu X, Liu J, Tong C, Fan HY (2017) Maternal DCAF2 is crucial for maintenance of genome stability during the first cell cycle in mice. *J Cell Sci* 130(19):3297–3307. <https://doi.org/10.1242/jcs.206664>
- Zhang J, Zhang YL, Zhao LW, Guo JX, Yu JL, Ji SY, Cao LR, Zhang SY, Shen L, Ou XH, Fan HY (2018) Mammalian nucleolar protein DCAF13 is essential for ovarian follicle maintenance and oocyte growth by mediating rRNA processing. *Cell Death Differ*. <https://doi.org/10.1038/s41418-018-0203-7>
- Zhang YL, Zhao LW, Zhang J, Le R, Ji SY, Chen C, Gao Y, Li D, Gao S, Fan HY (2018) DCAF13 promotes pluripotency by negatively regulating SUV39H1 stability during early embryonic development. *EMBO J*. <https://doi.org/10.15252/embj.201898981>
- Sha QQ, Dai XX, Jiang JC, Yu C, Jiang Y, Liu J, Ou XH, Zhang SY, Fan HY (2018) CFP1 coordinates histone H3 lysine-4 trimethylation and meiotic cell cycle progression in mouse oocytes. *Nat Commun* 9(1):3477. <https://doi.org/10.1038/s41467-018-05930-x>
- Zhang YL, Liu XM, Ji SY, Sha QQ, Zhang J, Fan HY (2015) ERK1/2 activities are dispensable for oocyte growth but are required for meiotic maturation and pronuclear formation in mouse. *J Genet Genomics* 42(9):477–485. <https://doi.org/10.1016/j.jgg.2015.07.004>
- Zhang Y, Yan Z, Qin Q, Nisenblat V, Chang HM, Yu Y, Wang T, Lu C, Yang M, Yang S, Yao Y, Zhu X, Xia X, Dang Y, Ren Y, Yuan P, Li R, Liu P, Guo H, Han J, He H, Zhang K, Wang Y, Wu Y, Li M, Qiao J, Yan J, Yan L (2018) Transcriptome landscape of human folliculogenesis reveals oocyte and granulosa cell interactions. *Mol Cell*. <https://doi.org/10.1016/j.molcel.2018.10.029>
- Brunet S, Dumont J, Lee KW, Kinoshita K, Hikal P, Gruss OJ, Maro B, Verlhac MH (2008) Meiotic regulation of TPX2 protein levels governs cell cycle progression in mouse oocytes. *PLoS One* 3(10):e3338. <https://doi.org/10.1371/journal.pone.0003338>
- Wang WH, Sun QY (2006) Meiotic spindle, spindle checkpoint and embryonic aneuploidy. *Front Biosci* 11:620–636

27. Sanders JR, Jones KT (2018) Regulation of the meiotic divisions of mammalian oocytes and eggs. *Biochem Soc Trans* 46(4):797–806. <https://doi.org/10.1042/BST20170493>
28. Tischer T, Schuh M (2016) The phosphatase Dusp7 drives meiotic resumption and chromosome alignment in mouse oocytes. *Cell Rep* 17(5):1426–1437. <https://doi.org/10.1016/j.celrep.2016.10.007>
29. Mihajlovic AI, FitzHarris G (2018) Segregating chromosomes in the mammalian oocyte. *Curr Biol* 28(16):R895–R907. <https://doi.org/10.1016/j.cub.2018.06.057>
30. Susor A, Jansova D, Cerna R, Danylevska A, Anger M, Toralova T, Malik R, Supolikova J, Cook MS, Oh JS, Kubelka M (2015) Temporal and spatial regulation of translation in the mammalian oocyte via the mTOR-eIF4F pathway. *Nat Commun* 6:6078. <https://doi.org/10.1038/ncomms7078>
31. Jansova D, Koncicka M, Tetkova A, Cerna R, Malik R, Del Llano E, Kubelka M, Susor A (2017) Regulation of 4E-BP1 activity in the mammalian oocyte. *Cell Cycle* 16(10):927–939. <https://doi.org/10.1080/15384101.2017.1295178>
32. Adhikari D, Liu K (2014) The regulation of maturation promoting factor during prophase I arrest and meiotic entry in mammalian oocytes. *Mol Cell Endocrinol* 382(1):480–487. <https://doi.org/10.1016/j.mce.2013.07.027>
33. Lincoln AJ, Wickramasinghe D, Stein P, Schultz RM, Palko ME, De Miguel MP, Tassarollo L, Donovan PJ (2002) Cdc25b phosphatase is required for resumption of meiosis during oocyte maturation. *Nat Genet* 30(4):446–449. <https://doi.org/10.1038/ng856>
34. Lan ZJ, Xu X, Cooney AJ (2004) Differential oocyte-specific expression of Cre recombinase activity in GDF-9-iCre, Zp3cre, and Msx2Cre transgenic mice. *Biol Reprod* 71(5):1469–1474. <https://doi.org/10.1095/biolreprod.104.031757>
35. Hein MY, Hubner NC, Poser I, Cox J, Nagaraj N, Toyoda Y, Gak IA, Weisswange I, Mansfeld J, Buchholz F, Hyman AA, Mann M (2015) A human interactome in three quantitative dimensions organized by stoichiometries and abundances. *Cell* 163(3):712–723. <https://doi.org/10.1016/j.cell.2015.09.053>
36. Reddy P, Liu L, Adhikari D, Jagarlamudi K, Rajareddy S, Shen Y, Du C, Tang W, Hamalainen T, Peng SL, Lan ZJ, Cooney AJ, Huhtaniemi I, Liu K (2008) Oocyte-specific deletion of Pten causes premature activation of the primordial follicle pool. *Science* 319(5863):611–613. <https://doi.org/10.1126/science.1152257>
37. Li J, Kawamura K, Cheng Y, Liu S, Klein C, Liu S, Duan EK, Hsueh AJ (2010) Activation of dormant ovarian follicles to generate mature eggs. *Proc Natl Acad Sci USA* 107(22):10280–10284. <https://doi.org/10.1073/pnas.1001198107>
38. Chen J, Torcia S, Xie F, Lin CJ, Cakmak H, Franciosi F, Horner K, Onodera C, Song JS, Cedars MI, Ramalho-Santos M, Conti M (2013) Somatic cells regulate maternal mRNA translation and developmental competence of mouse oocytes. *Nat Cell Biol* 15(12):1415–1423. <https://doi.org/10.1038/ncb2873>
39. Han SJ, Vaccari S, Nedachi T, Andersen CB, Kovacina KS, Roth RA, Conti M (2006) Protein kinase B/Akt phosphorylation of PDE3A and its role in mammalian oocyte maturation. *EMBO J* 25(24):5716–5725. <https://doi.org/10.1038/sj.emboj.7601431>
40. Chen Z, Zhang W, Jiang K, Chen B, Wang K, Lao L, Hou C, Wang F, Zhang C, Shen H (2018) MicroRNA-300 regulates the ubiquitination of PTEN through the CRL4B(DCAF13) E3 ligase in osteosarcoma cells. *Mol Ther Nucleic Acids* 10:254–268. <https://doi.org/10.1016/j.omtn.2017.12.010>
41. Kalous J, Solc P, Baran V, Kubelka M, Schultz RM, Motlik J (2006) PKB/AKT is involved in resumption of meiosis in mouse oocytes. *Biol Cell* 98(2):111–123. <https://doi.org/10.1042/BC20050020>
42. Sha QQ, Yu JL, Guo JX, Dai XX, Jiang JC, Zhang YL, Yu C, Ji SY, Jiang Y, Zhang SY, Shen L, Ou XH, Fan HY (2018) CNOT6L couples the selective degradation of maternal transcripts to meiotic cell cycle progression in mouse oocyte. *EMBO J*. <https://doi.org/10.15252/embj.201899333>
43. Jansen R, Tollervey D, Hurt EC (1993) A U3 snoRNP protein with homology to splicing factor PRP4 and G beta domains is required for ribosomal RNA processing. *EMBO J* 12(6):2549–2558
44. Liu Y, Zhao LW, Shen JL, Fan HY, Jin Y (2019) Maternal DCAF13 regulates chromatin tightness to contribute to embryonic development. *Sci Rep* 9(1):6278. <https://doi.org/10.1038/s41598-019-42179-w>
45. Kalous J, Tetkova A, Kubelka M, Susor A (2018) Importance of ERK1/2 in regulation of protein translation during oocyte meiosis. *Int J Mol Sci* 19:3. <https://doi.org/10.3390/ijms19030698>
46. Hoshino Y, Sato E (2008) Protein kinase B (PKB/Akt) is required for the completion of meiosis in mouse oocytes. *Dev Biol* 314(1):215–223. <https://doi.org/10.1016/j.ydbio.2007.12.005>
47. Tomek W, Smiljakovic T (2005) Activation of Akt (protein kinase B) stimulates metaphase I to metaphase II transition in bovine oocytes. *Reproduction* 130(4):423–430. <https://doi.org/10.1530/rep.1.00754>
48. El Sheikh M, Mesalam A, Mesalam AA, Idrees M, Lee KL, Kong IK (2019) Melatonin abrogates the anti-developmental effect of the AKT inhibitor SH6 in bovine oocytes and embryos. *Int J Mol Sci* 20:12. <https://doi.org/10.3390/ijms20122956>
49. Feitosa WB, Morris PL (2018) SUMOylation regulates germinal vesicle breakdown and the Akt/PKB pathway during mouse oocyte maturation. *Am J Physiol Cell Physiol* 315(1):C115–C121. <https://doi.org/10.1152/ajpcell.00038.2018>
50. Liu L, Li S, Li H, Yu D, Li C, Li G, Cao Y, Feng C, Deng X (2018) Protein kinase Cdelta (PKCdelta) involved in the regulation of pAkt1 (Ser473) on the release of mouse oocytes from diplotene arrest. *Cell Biochem Funct* 36(4):221–227. <https://doi.org/10.1002/cbf.3334>
51. Cao J, Hou P, Chen J, Wang P, Wang W, Liu W, Liu C, He X (2017) The overexpression and prognostic role of DCAF13 in hepatocellular carcinoma. *Tumour Biol* 39(6):1010428317705753. <https://doi.org/10.1177/1010428317705753>
52. Adhikari D, Liu K (2009) Molecular mechanisms underlying the activation of mammalian primordial follicles. *Endocr Rev* 30(5):438–464. <https://doi.org/10.1210/er.2008-0048>
53. Zheng W, Nagaraju G, Liu Z, Liu K (2012) Functional roles of the phosphatidylinositol 3-kinases (PI3Ks) signaling in the mammalian ovary. *Mol Cell Endocrinol* 356(1–2):24–30. <https://doi.org/10.1016/j.mce.2011.05.027>
54. Reddy P, Adhikari D, Zheng W, Liang S, Hamalainen T, Tohonen V, Ogawa W, Noda T, Volarevic S, Huhtaniemi I, Liu K (2009) PDK1 signaling in oocytes controls reproductive aging and lifespan by manipulating the survival of primordial follicles. *Hum Mol Genet* 18(15):2813–2824. <https://doi.org/10.1093/hmg/ddp217>

Publisher's Note Springer Nature remains neutral with regard to jurisdictional claims in published maps and institutional affiliations.

Terms and Conditions

Springer Nature journal content, brought to you courtesy of Springer Nature Customer Service Center GmbH (“Springer Nature”).

Springer Nature supports a reasonable amount of sharing of research papers by authors, subscribers and authorised users (“Users”), for small-scale personal, non-commercial use provided that all copyright, trade and service marks and other proprietary notices are maintained. By accessing, sharing, receiving or otherwise using the Springer Nature journal content you agree to these terms of use (“Terms”). For these purposes, Springer Nature considers academic use (by researchers and students) to be non-commercial.

These Terms are supplementary and will apply in addition to any applicable website terms and conditions, a relevant site licence or a personal subscription. These Terms will prevail over any conflict or ambiguity with regards to the relevant terms, a site licence or a personal subscription (to the extent of the conflict or ambiguity only). For Creative Commons-licensed articles, the terms of the Creative Commons license used will apply.

We collect and use personal data to provide access to the Springer Nature journal content. We may also use these personal data internally within ResearchGate and Springer Nature and as agreed share it, in an anonymised way, for purposes of tracking, analysis and reporting. We will not otherwise disclose your personal data outside the ResearchGate or the Springer Nature group of companies unless we have your permission as detailed in the Privacy Policy.

While Users may use the Springer Nature journal content for small scale, personal non-commercial use, it is important to note that Users may not:

1. use such content for the purpose of providing other users with access on a regular or large scale basis or as a means to circumvent access control;
2. use such content where to do so would be considered a criminal or statutory offence in any jurisdiction, or gives rise to civil liability, or is otherwise unlawful;
3. falsely or misleadingly imply or suggest endorsement, approval, sponsorship, or association unless explicitly agreed to by Springer Nature in writing;
4. use bots or other automated methods to access the content or redirect messages
5. override any security feature or exclusionary protocol; or
6. share the content in order to create substitute for Springer Nature products or services or a systematic database of Springer Nature journal content.

In line with the restriction against commercial use, Springer Nature does not permit the creation of a product or service that creates revenue, royalties, rent or income from our content or its inclusion as part of a paid for service or for other commercial gain. Springer Nature journal content cannot be used for inter-library loans and librarians may not upload Springer Nature journal content on a large scale into their, or any other, institutional repository.

These terms of use are reviewed regularly and may be amended at any time. Springer Nature is not obligated to publish any information or content on this website and may remove it or features or functionality at our sole discretion, at any time with or without notice. Springer Nature may revoke this licence to you at any time and remove access to any copies of the Springer Nature journal content which have been saved.

To the fullest extent permitted by law, Springer Nature makes no warranties, representations or guarantees to Users, either express or implied with respect to the Springer nature journal content and all parties disclaim and waive any implied warranties or warranties imposed by law, including merchantability or fitness for any particular purpose.

Please note that these rights do not automatically extend to content, data or other material published by Springer Nature that may be licensed from third parties.

If you would like to use or distribute our Springer Nature journal content to a wider audience or on a regular basis or in any other manner not expressly permitted by these Terms, please contact Springer Nature at

onlineservice@springernature.com